Muscle Velocity and Inertial Force From Phase Contrast MRI

Andrew L. Wentland, PhD,[1] Emily J. McWalter, PhD,[2] Saikat Pal, PhD,[3] Scott L. Delp, PhD,[4] and Garry E. Gold, MD[2,4]*

Purpose: To evaluate velocity waveforms in muscle and to create a tool and algorithm for computing and analyzing muscle inertial forces derived from 2D phase contrast (PC) magnetic resonance imaging (MRI).
Materials and Methods: PC MRI was performed in the forearm of four healthy volunteers during 1 Hz cycles of wrist flexion-extension as well as in the lower leg of six healthy volunteers during 1 Hz cycles of plantarflexion-dorsiflexion. Inertial forces (F) were derived via the equation $F = ma$. The mass, m, was derived by multiplying voxel volume by voxel-by-voxel estimates of density via fat-water separation techniques. Acceleration, a, was obtained via the derivative of the PC MRI velocity waveform.
Results: Mean velocities in the flexors of the forearm and lower leg were 1.94 ± 0.97 cm/s and 5.57 ± 2.72 cm/s, respectively, as averaged across all subjects; the inertial forces in the flexors of the forearm and lower leg were $1.9 \times 10^{-3} \pm 1.3 \times 10^{-3}$ N and $1.1 \times 10^{-2} \pm 6.1 \times 10^{-3}$ N, respectively, as averaged across all subjects.
Conclusion: PC MRI provided a promising means of computing muscle velocities and inertial forces—providing the first method for quantifying inertial forces.

J. MAGN. RESON. IMAGING 2015;42:526–532.

Two-dimensional (2D) phase contrast (PC) magnetic resonance imaging (MRI) is primarily used in cardiovascular imaging, as it allows for the acquisition of both anatomic and functional hemodynamic information.[1] Clinically, 2D PC MRI provides the ability to compute blood velocity and flow, pressure gradients across stenoses, cardiac output, and other cardiovascular parameters.[2] 2D PC MRI is available on nearly all scanner platforms.

The application of PC MRI to the evaluation of dynamic muscle motion and the quantification of muscle velocities has been underutilized. Previous studies on muscle velocity imaging have focused on the ability of the technique to provide information for biomechanical models, which in turn is useful for presurgical planning. Drace and Pelc[3,4] were the first to demonstrate that 2D PC MRI could be used to quantify muscle velocity in the forearm and lower leg. Further work has shown that muscle displacement,[5–7] strain,[8,9] and kinematics[10] can be evaluated from PC MRI data.[11] The quantification of muscle velocities and other derived values may provide useful diagnostic information on functional muscle deficits or focal areas of muscle hypokinesia, as in patients with neuromuscular disorders, muscle trauma, or muscle denervation.

In addition to using PC MRI to quantify muscle velocity, displacement, and strain, it may be possible to derive additional information, such as inertial force, which is the product of muscle mass and acceleration as determined by Newton's second law. Inertial forces are also referred to as fictitious forces. The magnitude of inertial forces is assumed to be negligible in biomechanical models,[12] although the validity of this assumption has not been demonstrated experimentally.

The purpose of this study was to evaluate velocity waveforms in muscle and to create a novel tool and algorithm for computing and analyzing inertial forces of muscle derived from 2D PC MRI. We reasoned that muscle inertial forces could be computed via MRI-derived estimates of muscle mass and acceleration. We hypothesized that the

View this article online at wileyonlinelibrary.com. DOI: 10.1002/jmri.24807

Received Sep 11, 2014, Accepted for publication Nov 4, 2014.

*Address reprint requests to: G.E.G., Stanford University School of Medicine, Department of Radiology, Lucas Center, P-271, 1201 Welch Rd., Stanford, CA 94305. E-mail: gold@stanford.edu

From the [1]Department of Medical Physics, University of Wisconsin School of Medicine & Public Health, Madison, Wisconsin, USA; [2]Department of Radiology, Stanford University School of Medicine, Stanford, California, USA; [3]Department of Biomedical Engineering, California Polytechnic State University, San Luis Obispo, California, USA; and [4]Department of Bioengineering, Stanford University School of Medicine, Stanford, California, USA

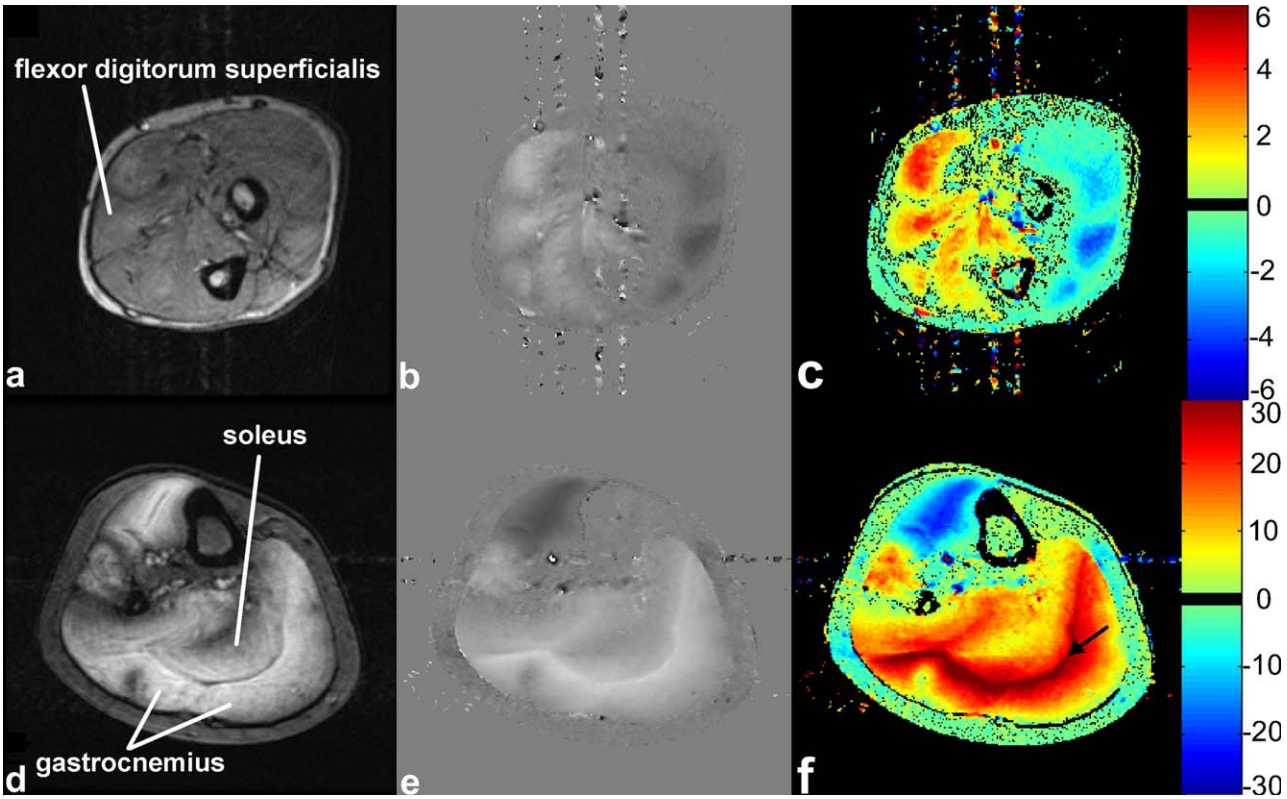

FIGURE 1: Cross-sectional 2D PC images of a forearm (a–c) and lower leg (d–f). Magnitude images (a,d), super-to-inferior through-plane velocity-encoded phase difference images with a magnitude mask (b,e), and color maps of the velocity-encoded phase difference images (c,f) are shown. Velocities are in cm/s. In the lower leg, velocities tended to be greatest at the junction of the gastrocnemius and soleus muscles (f, arrow).

muscle inertial forces would be orders of magnitude smaller than the active forces developed by muscle contraction to actuate the movement.

MATERIALS AND METHODS

Subjects

For imaging of the forearm, four healthy volunteers (three males, one female; mean age ± 1 SD = 30 ± 2.9 years) were included in this study. For imaging of the lower legs, six healthy volunteers (four males, two females; mean age ± 1 SD = 29.7 ± 4.5 years) were included in this study. This Health Insurance Portability and Accountability Act (HIPAA)-compliant study was approved by our Institutional Human Subjects Review Committee and written informed consent was obtained from all subjects.

Imaging

Imaging was performed on a 3.0T MRI system (Discovery 750, GE Healthcare, Waukesha, WI) using an eight-channel phased array cardiac coil. Axial or coronal images of the forearms and lower legs were imaged with IDEAL (Iterative Decomposition of water and fat with Echo Asymmetry and Least squares estimation)[13,14] using the following parameters: TR/TE/flip = 6.0/3.0 msec/30° pixel bandwidth (BW) =976.6 Hz, field of view (FOV) = 14 cm (arm) or 26 cm (leg), slice thickness = 6 mm, 256 × 256 matrix, and 5.6-second scan time per slice. Separate fat and water images were generated during the reconstruction. Both axial and coronal IDEAL slices were prescribed in a series that covered the entire volume of the forearm or lower leg. 2D PC imaging with retrospective gating[15] was acquired with the following parameters: TR/TE/flip = 18.0/7.1 msec/20° pixel BW = 122.1 Hz, FOV = 14 cm (arm) or 26 cm (leg), slice thickness = 6 mm, 256 × 256 matrix, and velocity encoding of 10 cm/s (arm) or 40 cm/s (leg); view-sharing[16] was employed to reconstruct to 32 time frames. The scan time was 170 seconds. Axial PC slices were acquired with through-plane velocity encoding; coronal PC slices were acquired with in-plane superior-to-inferior velocity encoding. Axial PC slices were prescribed at 30% of the proximal distance from the elbow to the wrist joints and at 30% of the proximal distance from the knee to the ankle joints. Axial PC slices were prescribed at the same location as one of the axial IDEAL slices for subsequent computation of inertial forces, as described below. Coronal PC images were prescribed at the widest portion of the forearm and lower leg as identified by the IDEAL series.

For imaging of the forearm, subjects were either in a prone or lateral decubitus position. For imaging of the lower leg, subjects were in a supine position. During the acquisition of PC images a metronome set to 1 Hz was played over headphones provided to each subject. A high tone indicated that a subject's hand or foot should be in the neutral position; at the halfway point of the 1 Hz cycle a low tone indicated that a subject's hand or foot should be at the maximum point of flexion or plantarflexion, respectively. Simultaneously, an electrocardiogram waveform generator was interfaced with the MR scanner to provide a 1 Hz signal for gating

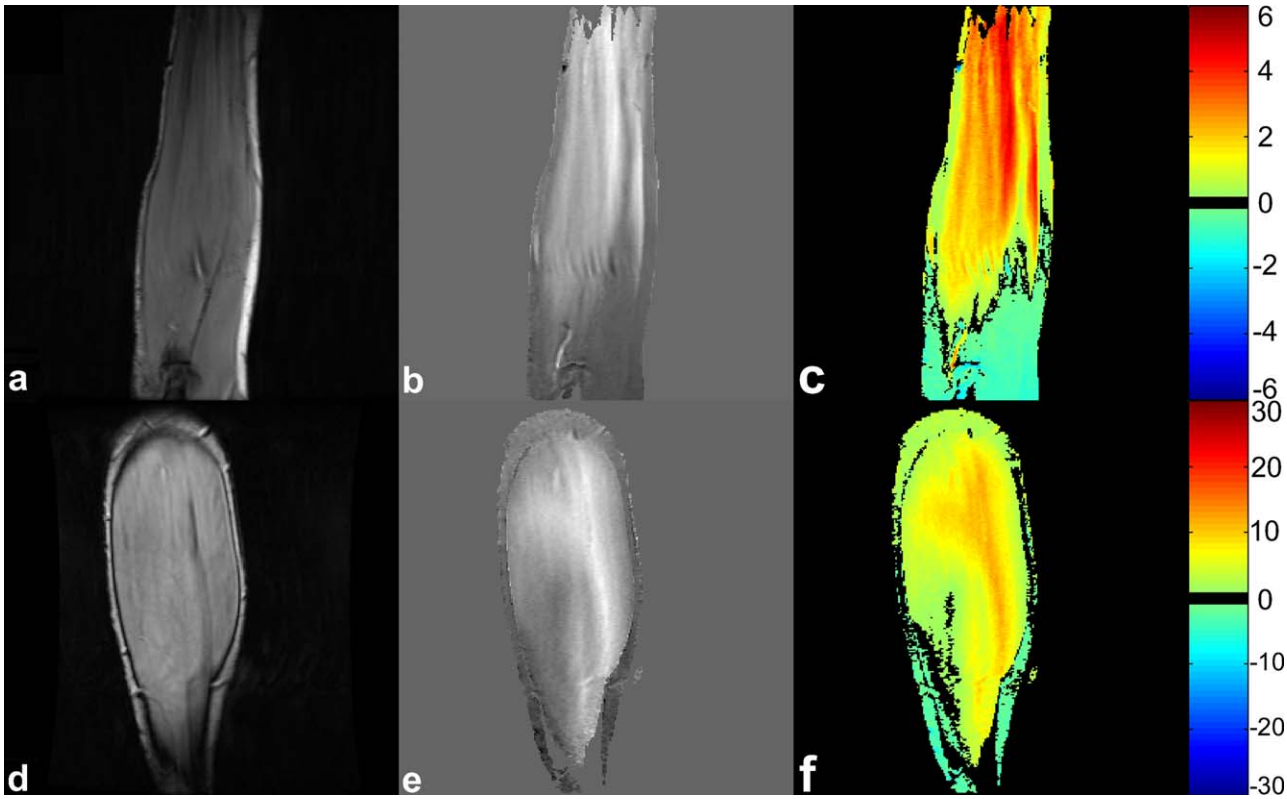

FIGURE 2: Coronal images of the forearm (a–c) and lower leg (d–f). Magnitude images (a,d), super-to-inferior through-plane velocity-encoded phase difference images with a magnitude mask (b,e), and color maps of the velocity-encoded phase difference images (c,f) are shown. Velocities are in cm/s.

to the motion cycle during the PC acquisition. Subjects repeated the neutral-flexion-neutral cycle once per second for the duration of the 170-second 2D PC MRI acquisition. A tension band was held in the hand or wrapped around the foot during each experiment to provide resistance. To improve the consistency of the motion cycle in the wrist, a board was constructed with pegs to provide stopping points, such that the dorsal surface of the hand hit one peg during the neutral phase of the motion cycle and the other side of the hand hit another peg during the flexed phase of the motion cycle. No such board or stopping points were used in the acquisition of images in the lower leg. In addition to imaging the forearms and lower leg in both the coronal and axial planes, three bands of different stiffness were tested under identical experimental conditions in the forearm. The bands would allow us to distinguish whether our computed forces were representative of inertial or active force. If active force was being measured, we would expect significant changes in the magnitude of the force and the force waveforms with each of the different bands. If inertial force was being measured, we would expect minimal changes in the computed force values with each of the different bands.

Derivation of Inertial Force

The computation of inertial force required that both acceleration and mass be determined on a per-voxel basis. First, the velocity waveform of each voxel over the motion cycle was smoothed with a Savitzky-Golay filter.[17] An acceleration waveform was then computed from the smoothed velocity waveform via the first-order finite difference. For the estimation of the mass of each voxel a density map was created from the IDEAL images via a weighted average of the signal from the fat and water images, assuming muscle density is 1.06 g/mL[18] and fat density is 0.9 g/mL.[19] A mass map was created by multiplying the estimated density of each voxel by the known voxel volume. Inertial force over the motion cycle was computed by multiplying the mass by the acceleration waveform for each voxel.

Data Analysis

A custom MatLab-based graphical user interface (MathWorks, Natick, MA) was created to automate the process of loading fat/water images, computing density and mass maps, loading PC images, deriving acceleration, and computing inertial forces. For analysis, regions of interest (ROIs) were drawn on axial images over the entire region of the wrist flexors and foot plantarflexors for all subjects. From the ROIs the graphical user interface computed the summed inertial force and the average and standard deviation (SD) of velocity over the entire motion cycle. Average velocity and inertial force values for all subjects were reported for the peak timepoint of the flexion phase of the motion cycle. Velocity and inertial force waveforms were compared graphically for the experiment comparing three stiffness bands. To demonstrate the distribution of velocity values within a cross-section of muscle, histograms were created for velocity values over the axial area of the medial and lateral gastrocnemius muscles for the neutral and peak contraction and relaxation phases of the motion cycle. Color maps were applied to the PC images to assess for variations in velocity values across the muscles.

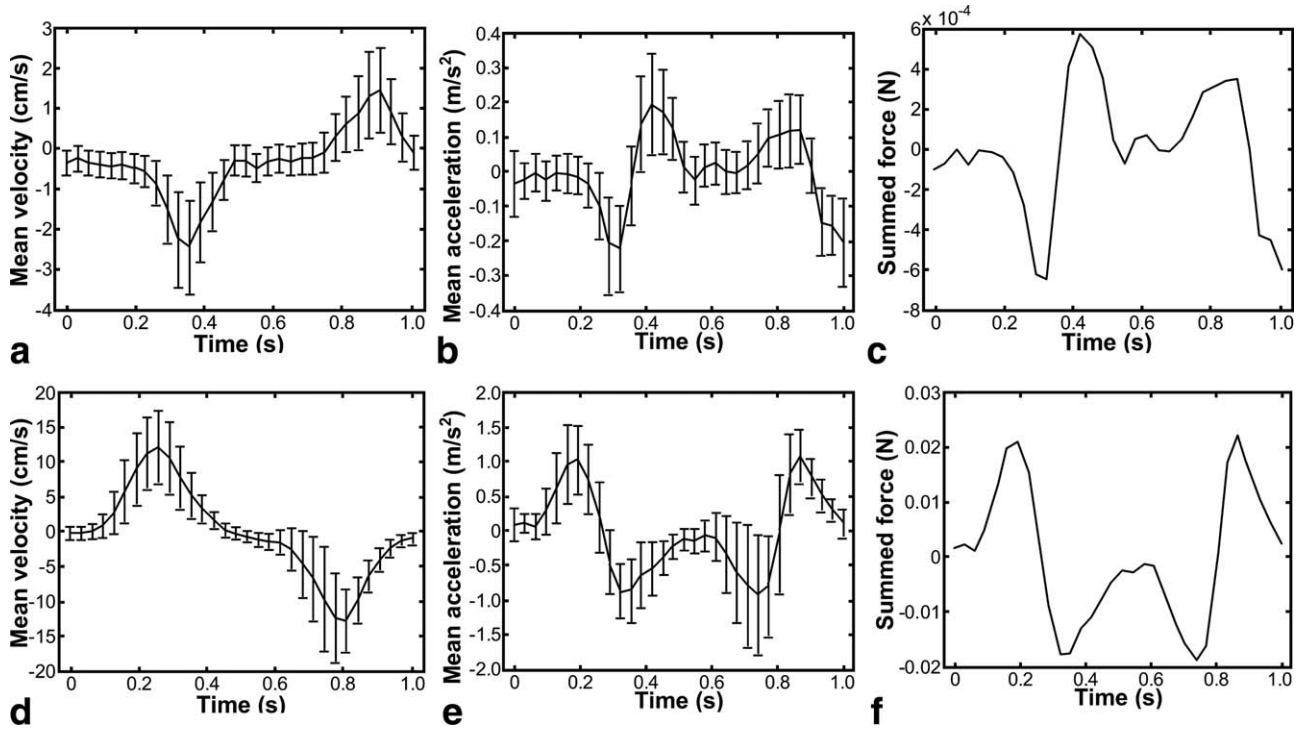

FIGURE 3: Representative velocity, acceleration, and inertial force waveforms derived from an ROI) drawn on a cross-section of the flexor digitorum superficialis muscle (a–c) and the gastrocnemius muscle (d–f). Mean velocity (±1 SD) (a,d), mean acceleration (±1 SD) (b,e), and inertial force (c,f) summed over the ROI are shown for all 32 time frames over the 1 Hz motion cycle.

RESULTS

Imaging of wrist flexion and plantarflexion motion cycles with PC MRI provided images without appreciable motion artifact in all subjects (A.L.W.). Figures 1 and 2 show representative images in the forearm and lower leg. Color maps of the velocity-encoded images (Fig. 1c,f) demonstrated that velocity values tended to be greatest in the middle of the muscle bellies in the forearm, whereas velocities in the lower leg tended to be greatest at the junction of the gastrocnemius and soleus muscles. Coronally oriented PC images with superior-to-inferior in-plane velocity encoding demonstrated a relatively uniform distribution of velocities in the superior-to-inferior direction, with appreciable variation in the medial-to-lateral direction (Fig. 2c). In comparison, images in the lower leg showed recognizable variation in velocities in both the superior-to-inferior and medial-to-lateral directions (Fig. 2f).

The magnitude of the velocity, acceleration, and inertial force waveforms were substantially larger in the medial and lateral gastrocnemius muscles than in the flexor digitorum superficialis muscle. During the peak contractile phase of a 1 Hz motion cycle, mean velocities in the flexors of the forearm (Fig. 1a–c) and lower leg (Fig. 1d–f) were 1.94 ± 0.97 cm/s and 5.57 ± 2.72 cm/s, respectively, as averaged across all subjects via axial slices; the summed inertial forces in the flexors of the forearm and lower leg were $1.9 \times 10^{-3} \pm 1.3 \times 10^{-3}$ N and $1.1 \times 10^{-2} \pm 6.1 \times$

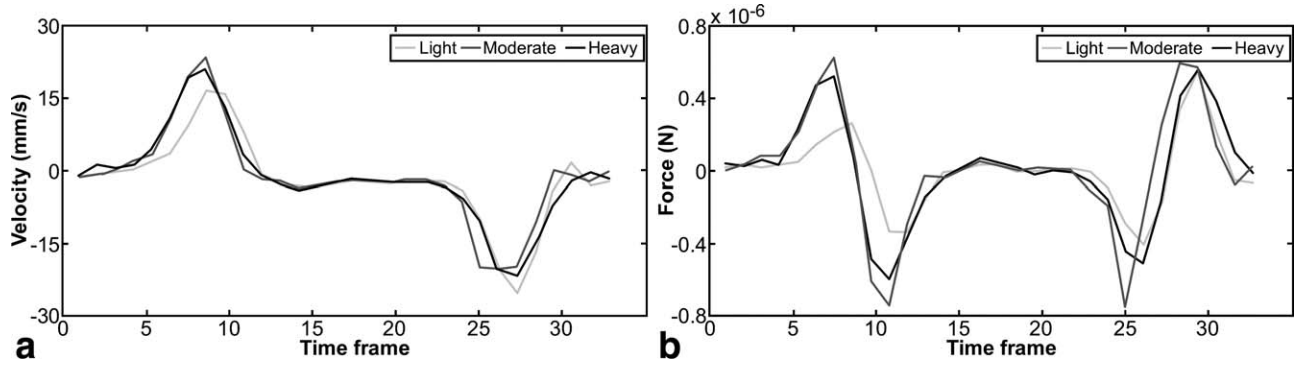

FIGURE 4: Velocity (a) and inertial force (b) waveforms in back-to-back experiments using physical therapy bands of varying stiffness. Waveforms are derived from an ROI drawn on a cross-section of the flexor digitorum superficialis muscle.

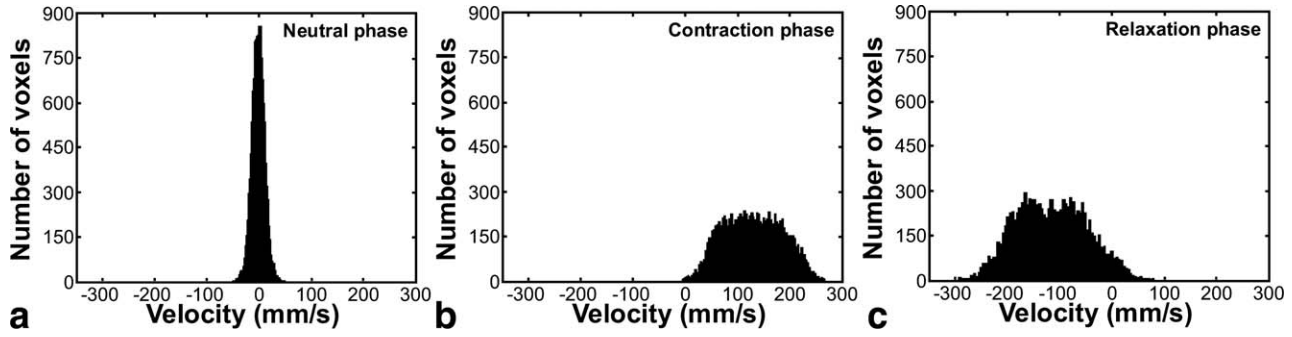

FIGURE 5: Histograms depicting the distribution of muscle velocities within a cross-section of the gastrocnemius muscle demonstrated substantial variability of muscle velocities during the peak contraction (b) and relaxation (c) phases of the motion cycle, relative to the neutral phase (a).

10^{-3} N, respectively, as averaged across all subjects. Representative velocity, acceleration, and inertial force waveforms over the motion cycle for the flexor digitorum superficialis muscle and the gastrocnemius muscle are shown in Fig. 3.

Representative velocity and inertial force waveforms for a subject repeating the PC MRI acquisition with varying stiffness bands are shown in Fig. 4. The magnitudes of the velocity and inertial force waveforms were similar between the moderate and heavy bands. During the contraction phase of the motion cycle, the magnitudes of the velocity and inertial force waveforms were lower in intensity for the band with the least stiffness as compared with the other bands.

Voxel-by-voxel analyses of muscle velocity were evaluated for the time-resolved PC MRI datasets (Fig. 5). Histograms of the voxel-by-voxel velocity analyses demonstrated a wide distribution of muscle velocities within muscle cross-sections, particularly during the peak contraction and relaxation phases of the motion cycle.

DISCUSSION

This study demonstrates that muscle motion can be evaluated with PC MRI via commercially available pulse sequences and a simple gating technique. These methods are widely available and can be applied on many different MRI systems. With the creation and application of postprocessing software, we are able to quantify inertial forces in muscle for the first time, which may be useful for studies of muscle motion in health and disease.

A previous study[5] used sophisticated optical tracking methods to gate the PC MRI acquisition with the motion cycle. Despite the simplicity of the gating method employed in our study, velocity waveforms of muscle motion had a distinct shape consistent with that expected by the bulk muscle motion; none of the subjects imaged had difficulty performing the motion and all acquired data were of sufficient technical quality for analysis.

Our technique for measuring inertial force uses Newton's second law, F = ma, and thus depends on the determination of muscle motion as detected with PC MRI. The proposed technique does not reflect what occurs on the muscle fiber or motor unit level; in other words, a muscle fiber can be in motion and be quantified in its inertial force with our technique, but our technique does not discriminate between muscle fibers that are or are not recruited (ie, some muscle fibers may be pulled along with muscle contraction but the myosin heads are not engaged). Active forces are generated by the recruitment of muscle fibers and are distinct from inertial forces. Therefore, the strength of muscle contraction and the resulting active forces are not represented in our technique. Our evaluation of velocity and inertial force with physical therapy bands of varying stiffness served to corroborate the hypothesis that our technique evaluates inertial force rather than active force, given that the change in inertial force from one band to another was small. Large variations in measured force with the physical therapy bands would have suggested that active force rather than inertial force was evaluated by our technique. Compared to the other two bands, the inertial forces associated with the least stiff band had a shifted waveform and lower magnitude during the contraction phase. Given the similarity between the waveforms and magnitudes for the other two bands, it is possible that the volunteers conducted the motion cycle differently with the least stiff band considering its relative laxity. It is important to note that identical bands were employed for each subject rather than using a band tailored to a percentage of each subject's maximal voluntary contraction; by using identical bands the force needed to stretch the bands is also identical. Using different bands between subjects could obfuscate whether active or inertial forces were being evaluated.

It is noteworthy, but not surprising, that the magnitudes of inertial forces are small. Inertial forces are assumed to be negligible in biomechanical models. It should be noted that the force values provided in this study are only valid for the region of interest and therefore the mass associated with the region of interest on a single slice. To compute the inertial force for an entire muscle, the velocity

along the entire muscle as well as the mass of the entire muscle would need to be evaluated. Nevertheless, given that the reported inertial force values are on the order of a milli-Newton or less in magnitude, even a muscle weighing several kilograms would still only produce a summed inertial force of a few Newtons. Furthermore, our measured inertial forces are orders of magnitude smaller than the reported maximum force generating capacities of muscle. For example, the gastrocnemius has a maximum force generating capacity of 600–1300 N,[20] which is considerably greater than our measured inertial forces.

Currently, PC MRI is not a standard diagnostic method for evaluating muscle motion. However, such an evaluation may provide useful diagnostic information on functional muscle deficits or focal areas of muscle hypokinesia, as in patients with neuromuscular disorders, muscle trauma, or muscle denervation. One clinical study of muscle motion used PC MRI to determine whether or not the rectus femoris muscle was converted from a knee extensor to a knee flexor after tendon transfer surgery.[7] As shown in our study, histogram analysis of muscle motion demonstrates that there is a range of velocities within the cross-section of a given muscle; in biomechanical models entire muscles are assumed to move with the same speed. Yet Pappas et al[6] demonstrated with PC MRI that the biceps brachii muscle shortens nonuniformly during elbow flexion. PC MRI therefore provides unique physiologic information of muscle motion that may prove useful for refining biomechanical models. For example, in this study we observed that velocities in the lower leg tended to be greatest at the junction of the gastrocnemius and soleus muscles. High shear has been detected in the aponeuroses between these muscles,[21] which suggests that these two muscles are sufficiently separate from one another to account for the elevated velocity at the muscle junction. In comparison, velocity tended to be greatest in the middle of the muscle bellies in the forearm, which is likely due to tethering of the muscle edges to the surrounding tissue.

There are a number of limitations in this study. Our evaluation of muscle velocities and inertial forces are limited to actions that can be performed in the MRI scanner bore, as well as by the limited speed with which subjects can complete motion cycles. In our experiments, attempts were made to perform motion cycles at 2 and 3 Hz rather than 1 Hz, but this proved to be difficult for subjects to perform. As such, the 1 Hz motion cycles presented in this study are likely unrepresentative of muscle velocities and inertial forces that would typically apply to biomechanical models. However, given the low magnitude of our measured velocity and inertial force values, it is reasonable to assume that values would still be relatively low in magnitude within the physiological range of muscle motion. Another limitation is in regard to the calculation of acceleration; acceleration encoding with MRI is possible[22] and would avoid the need to derive acceleration waveforms from velocity waveforms, as was employed in this study. However, acceleration-encoded acquisitions are not commercially available; in this study we sought to use only techniques that were readily available. Acquisition time was cumbersome in this study; retrospectively gated acquisitions are time-consuming but provide the advantage of capturing the entire motion cycle rather than using a trigger delay that leads to missed portions of the motion cycle (as with prospectively gated acquisitions). Long scan times are potentially problematic should PC MRI be used to evaluate muscular deficiencies in patients, given the fatigue experienced by our normal subjects over the 170-second scan time; patients are less likely to be able to tolerate such a scan time. In future work it is possible to employ a radially undersampled PC acquisition with retrospective gating,[23] which has a scan time on the order of ~30 seconds; however, such a technique is not commercially available at this time. Finally, there is no reference or gold standard by which we can compare the results of this study; while the accuracy of 2D PC MRI techniques has been well-validated,[24] our method is the first known method for quantifying inertial forces and therefore has no technique by which it can be compared or validated.

Our study employed a one-directional 2D PC MRI acquisition, which can capture only a single component of the complex 3D contraction of muscle. Techniques are available that provide three-directional velocity encoding for every point within a volumetric dataset for every timepoint during a motion cycle (so-called 4D PC MRI); therefore, it would be possible to elicit velocity in all three directions for the entire forearm or entire lower leg during a motion cycle. Such acquisitions are currently available on some scanner platforms, but the acquisition time is a severe limitation. Even with undersampling methods, three-directional volumetric PC MRI acquisitions require at least 7–10 minutes of scan time, depending on the imaging parameters.[25] While it may be difficult to utilize such a lengthy acquisition to evaluate muscle motion in a clinical setting, it may prove useful for biomechanical applications.

In conclusion, 2D PC MRI provided a promising means of computing muscle velocities and inertial forces; additionally, our technique provides the first known method for quantifying inertial forces. Our analysis technique may be useful in evaluating muscle pathophysiology and further developing biomechanical models. Our results demonstrate that inertial forces are small in relation to active forces and may be ignored in cases of low load and slow movement.

Acknowledgment

Contract grant sponsor: NHLBI Ruth L. Kirschstein National Research Service Award for Individual Predoctoral

MD/PhD Fellows; Contract grant number: F30 HL108539-02; Contract grant sponsor: NIH Medical Scientist Training Program; Contract grant numbers: T32 GM008692, NIHEB002524, NIHAR062068; Contract grant sponsor: GE Healthcare.

References

1. Gatehouse PD, Keegan J, Crowe LA, et al. Applications of phase-contrast flow and velocity imaging in cardiovascular MRI. Eur Radiol 2005;15:2172–2184.
2. Caroff J, Biere L, Trebuchet G, et al. Applications of phase-contrast velocimetry sequences in cardiovascular imaging. Diagn Intervent Imaging 2012;93:159–170.
3. Drace JE, Pelc NJ. Measurement of skeletal muscle motion in vivo with phase-contrast MR imaging. J Magn Reson Imaging 1994;4:157–163.
4. Drace JE, Pelc NJ. Skeletal muscle contraction: analysis with use of velocity distributions from phase-contrast MR imaging. Radiology 1994;193:423–429.
5. Sheehan FT, Zajac FE, Drace JE. Using cine phase contrast magnetic resonance imaging to non-invasively study in vivo knee dynamics. J Biomech 1998;31:21–26.
6. Pappas GP, Asakawa DS, Delp SL, Zajac FE, Drace JE. Nonuniform shortening in the biceps brachii during elbow flexion. J Appl Physiol 2002;92:2381–2389.
7. Asakawa DS, Blemker SS, Gold GE, Delp SL. In vivo motion of the rectus femoris muscle after tendon transfer surgery. J Biomech 2002; 35:1029–1037.
8. Drace JE, Pelc NJ. Tracking the motion of skeletal muscle with velocity-encoded MR imaging. J Magn Reson Imaging 1994;4:773–778.
9. Sheehan FT, Drace JE. Human patellar tendon strain. A noninvasive, in vivo study. Clin Orthopaed Relat Res 2000:201–207.
10. Rebmann AJ, Sheehan FT. Precise 3D skeletal kinematics using fast phase contrast magnetic resonance imaging. J Magn Reson Imaging 2003;17:206–213.
11. Asakawa DS, Pappas GP, Blemker SS, Drace JE, Delp SL. Cine phase-contrast magnetic resonance imaging as a tool for quantification of skeletal muscle motion. Semin Musculoskel Radiol 2003;7:287–295.
12. Brinckmann P, Frobin W, Leivseth G. Musculoskeletal biomechanics. Stuttgart, Germany: Thieme: 2002.
13. Reeder SB, McKenzie CA, Pineda AR, et al. Water-fat separation with IDEAL gradient-echo imaging. J Magn Reson Imaging 2007;25:644–652.
14. Reeder SB, Wen Z, Yu H, et al. Multicoil Dixon chemical species separation with an iterative least-squares estimation method. Magn Reson Med 2004;51:35–45.
15. Lenz GW, Haacke EM, White RD. Retrospective cardiac gating: a review of technical aspects and future directions. Magn Reson Imaging 1989;7:445–455.
16. Markl M, Hennig J. Phase contrast MRI with improved temporal resolution by view sharing: k-space related velocity mapping properties. Magn Reson Imaging 2001;19:669–676.
17. Savitzky A, Golay MJE. Smoothing and differentiation of data by simplified least squares procedures. Anal Chem 1964;36:1627–1639.
18. Mendez J, Keys A. Density and composition of mammalian muscle. Metabolism 1960;9:184–188.
19. Abate N, Burns D, Peshock RM, Garg A, Grundy SM. Estimation of adipose tissue mass by magnetic resonance imaging: validation against dissection in human cadavers. J Lipid Res 1994;35:1490–1496.
20. Arnold EM, Ward SR, Lieber RL, Delp SL. A model of the lower limb for analysis of human movement. Ann Biomed Eng 2010;38:269–279.
21. Bojsen-Moller J, Hansen P, Aagaard P, Svantesson U, Kjaer M, Magnusson SP. Differential displacement of the human soleus and medial gastrocnemius aponeuroses during isometric plantar flexor contractions in vivo. J Appl Physiol 2004;97:1908–1914.
22. Tasu JP, Jolivet O, Mousseaux E, Delouche A, Diebold B, Bittoun J. Acceleration mapping by Fourier acceleration-encoding: in vitro study and initial results in the great thoracic vessels. Magn Reson Med 1997;38:110–116.
23. Wentland AL, Korosec FR, Vigen KK, Wieben O, Fine JP, Grist TM. Cine flow measurements using phase contrast with undersampled projections: in vitro validation and preliminary results in vivo. J Magn Reson Imaging 2006;24:945–951.
24. Rebergen SA, van der Wall EE, Doornbos J, de Roos A. Magnetic resonance measurement of velocity and flow: technique, validation, and cardiovascular applications. Am Heart J 1993;126:1439–1456.
25. Gu T, Korosec FR, Block WF, et al. PC VIPR: a high-speed 3D phase-contrast method for flow quantification and high-resolution angiography. AJNR Am J Neuroradiol 2005;26:743–749.